Materials Today: Proceedings 42 (2021) 2822–2828

Contents lists available at ScienceDirect

Materials Today: Proceedings

journal homepage: www.elsevier.com/locate/matpr

Simulation of thin-walled double hexagonal aluminium 5754 alloy foam-filled section subjected to direct and oblique loading

Samer Abdulqadir [a], Bassam Alaseel [b,*], M.N.M. Ansari [b,c]

[a] Department of Mechanical Engineering, University of Anbar, Iraq
[b] Mechanical Engineering Department, Universiti Tenaga National (UNITEN), 43000 Kajang, Malaysia
[c] Institute of Power Engineering, Universiti Tenaga National (UNITEN), 43000 Kajang, Malaysia

ARTICLE INFO

Article history:
Available online 16 February 2021

Keywords:
Dynamic
Energy absorption
Aluminium foam
Hexagonal
Doubles tube

ABSTRACT

This paper presents the numerical study of the dynamic loading on the thin-walled tube made of aluminium alloy. The non-linear finite element was used to simulate and to predict the crushing phenomenon of the structure subjected to dynamic loading. The study deals with the energy absorption of empty and aluminium foam-filled double thin-walled hexagonal tubes under axial crushing load. The specimen is a regular hexagonal tube which consists of an outer and inner tube. The outer tube was fixed at a perimeter of 360 mm with a side of 60 mm each. While different inner perimeters were used. The paper studied two types of structures, the empty double hexagonal tubes and foam-filled tubes. The multi-criteria decision making (MCDM) process, the complex proportional assessment method (COPRAS) was used to select the best specimen. Although it has 17% lower specific energy absorption, the specimen of inner side tube of 45 mm with foam (H-D-F) was the best crashworthiness performance was selected as the best one since it has 64% lower peal force, 33% higher in CFE and reduction in specimen mass by 30%.

Selection and peer-review under responsibility of the scientific committee of the 3rd International Conference on Materials Engineering & Science.

1. Introduction

Thin-walled tubes have been widely utilized as an energy absorber in vehicles, trains and even aerospace applications to protect the passengers during incidences due to the greater energy absorption capability easy manufacturing process and lightweight [1–3]. The function of the energy absorbers is to absorb energy due to collision after converting it from kinetic energy to plastic deformation energy this leads to reduce the number of fatalities and injuries. The crush force efficiency (CFE) is a crucial crashworthiness parameter to evaluate the performance of the crushed tubes [4]. The geometry of the energy absorber has a significant effect on the amount of energy absorption i.e. circular [5–6], square, hexagonal [7–8] and octagonal shape [9–10]. These geometries have been well studied analytically, numerically and experimentally in the past decades. From all these geometries, the hexagonal geometry has shown an excellent crashworthiness performance due to its deformation mode [11]. Tarlochan et al. [12] studied different thin-walled geometries subjected to an oblique loading. The study has found that the hexagonal cross-section has the best performance. Alkibr [13] studied experimentally kenaf fibre reinforced regular hexagonal tubes with different angles. The study has exhibited that the maximum specific energy absorption of the hexagonal tubes occurs at 60^0. Na Qiu et al. [14] investigated the crash performance multi-cell hexagonal profiles subjected to direct and oblique loads. The study found that the number of corners has an important role in improving energy absorption.

Sahil Goyal et al. [15] studied a different type of polygon cross-section to enhance energy absorption and crush force efficiency. The study showed that the specific energy absorption of a foam-filled polygon has 40% higher than the empty tube. Isabel Duarte et al. [16] studied foam-filled thin-walled tubes made of aluminium subjected to quasi-static and dynamic loads. The results showed that the deformation of the structure has enhanced due to foam and it prevented the global buckling of the structure. The study found that the energy absorption and specific energy absorption of foam-filled tubes have increased when compared with the empty tubes.

The current study aims to optimize the design that could be used as an alternative one instead of the conventional structure

* Corresponding author.
E-mail address: bsmaq.it@gmail.com (B. Alaseel).

https://doi.org/10.1016/j.matpr.2020.12.728
2214-7853/
Selection and peer-review under responsibility of the scientific committee of the 3rd International Conference on Materials Engineering & Science.

Fig. 1. Metallic coupon specimen dimensions for the quasi-static test.

which has the best crashworthiness performance by incorporated foam-filled double hexagonal tubes and also a chance to reduce the mass of the proposed design.

2. Materials and tube description

In this study, the double regular hexagonal tubes were made of 5754 aluminium alloy. The material properties used in this study were generated from the standard tensile testing of coupon. An Instron 5800R 100kN test machine has been used to test the specimens. The samples were tested under quasi-static with a speed of 2 mm/min Fig. 1. The modulus of elasticity of the material is E = 68 GPa, Yield stress is 60 MPa, Ultimate tensile stress is 190 MPa, the density is $\rho = 2700$ kg/m3 and the poison's ratio is $\nu = 0.3$. The strain rate in this study was neglected since aluminium is strain-rate independent.

The stress–strain data (Fig. 2) which was obtained from the stress–strain curve of the tested specimen by a static test illustrated in Table 1. The current study proposed a design which consists of a regular double hexagonal tube with and without aluminium foam. The outer tube perimeter was kept at 360 mm with a wall thickness of 2 mm and a length of 350 mm. while the different inner perimeter was studied. (330, 300, 270, 240, 210 and 180 mm) with a wall thickness of 1 mm and a tube length of 350 mm. The foam occupied the gap between the two tubes Fig. 3. Initially, the study runs the outer tube alone with and without foam. Then, the study moves on to simulate the rest of the specimens. 14 specimens are proposed in terms of different inner perimeters and empty and foam-filled specimen. All the specimen will be subjected to both direct and an oblique loading with a degree of 30. COPRAS method was used to select the best crashworthiness performance among them. Samples were identified using letters for better recognition. The first letter (H) denotes to the outer tube (hexagonal tube) while the second letter represents the inner tube. If the specimen has the letter (F) this means the specimen has foam otherwise, two letters means empty specimen.

3. Finite element simulation

The proposed model in this research is a double thin-walled hexagonal tube. The model consists of two concentric tubes. Both outer and inner tubes are regular hexagonal shape. The outer tube has a perimeter of 360 mm while different inner tube perimeters were considered. The non-linear finite element was used to simulate the specimens. The entire structure consists of a double tube, aluminium foam and two rigid plates. Both tubes were modelled as a quad element with 4 node shell elements (S4R) explicit, element deletion and enhanced hourglass. The element size is chosen at 5 mm. The contact used to simulate the interaction between all the structure parts were general contact and the coefficient of friction surfaces was 0.2 [8,17–19]. Both rigid plates were modelled as a rigid body. The bottom plate was constrained and fixed to move in all directions while the upper plate (striker) was permitted to move in the transitional displacement with the direction of the impact loading as shown in Fig. 4. The velocity of the striker was chosen from the New Car Assessment Program (NCAP) by the National Traffic Safety Administration (NHTSA) and it was modelled as 56 km/h. and the mass was 275 kg which represents 25% of the compact car. The double tube specimens which will be used as an energy absorber was assumed to absorb 50% of the impact energy during collision [12].

Table 1
Aluminium alloy properties.

Stress (σ) 'MPa'	Strain (ε) %
60	0
89	0.016
127	0.052
143	0.0782
152	0.0914
160	0.1071
170	0.1366
178	0.1623
186	0.213
190	0.254

4. Results and discussions

4.1. Direct impact

The deformation analysis of double regular hexagonal tubes and the effect of aluminium foam subjected to axial force was numerically investigated using ABAQUS software. The deformation modes of the double hexagonal tubes for foam-filled, partially filled and empty tubes are illustrated in Fig. 5. For foam filled tube, when the specimen loaded dynamically, the folds started from the end near the striker and continued as axisymmetric (concertina) folds and then began to form from the other end along the length of the specimen. The partial foam suffered from diamond folds which moving outward and inward due to the presence of foam. The empty tube buckled and generated deformation modes of

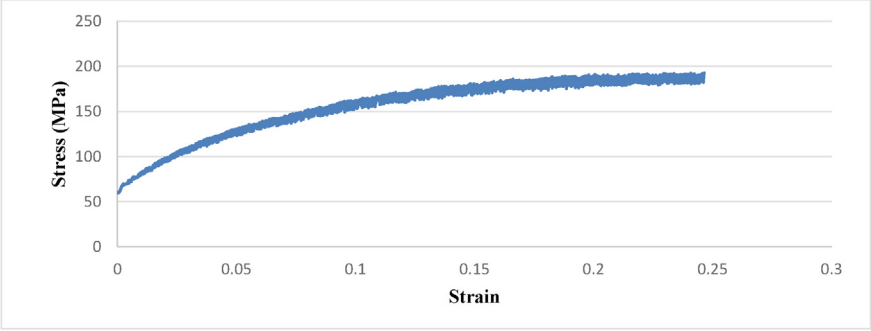

Fig. 2. Stress–strain curve for quasi-static tensile test for 5754.

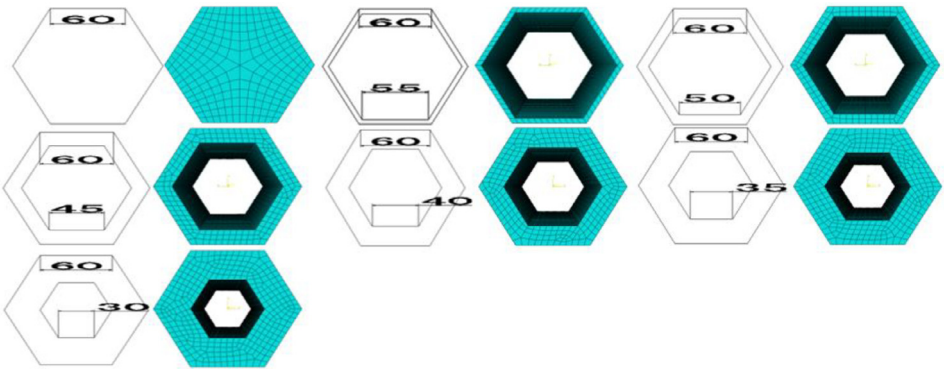

Fig. 3. Cross-sectional configurations of both double hexagonal tube and aluminium foam.

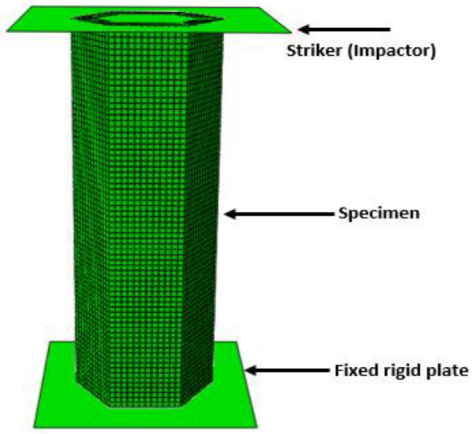

Fig. 4. Finite element analysis setup for the double hexagonal tube.

mixed-mode concertina and mixed-mode along the length of the specimen.

The force–displacement curves of the foam-filled and empty double hexagonal tubes in terms of direct loading are illustrated in Fig. 6 and Fig. 7 respectively. In the foam-filled specimen (Fig. 6), the initial peak forces are higher than those in empty tubes due to the presence of foam. Initially, the force increases rapidly when the impactor hits the structure. This force is needed to start the deformation and to form the first fold. When the first fold has created, the force begins to reduce and then increases again when another fold is formed. This fluctuation of the force will continue but the force increases with each fold formation due to the densification of the foam. These findings were significant in (H-F, H-A-F, H-B-F and H-C-F) specimens. It was noted that these changes were not substantial in (H-D-F, H-E-F and H-F-F) specimens due to less foam mass. Where there was a minimal fluctuation of the force during folds formation with the minimum difference between the initial and maximum force. It was noted that the specimen with the biggest foam mass (filled tube H-F) had the highest force, which is 399kN. This force decreases as foam mass reduces with the minimum force found at the specimen H-F-F which is 100kN. The ratio between the average force and the maximum force is referred to as the crush force efficiency (CFE). The higher the CFE, the better the performance.

The specimen H-D-F shows an almost steady curve after the initial force with no high fluctuations and no significant difference between the peak force and the average force. Therefore, the H-D-F specimen had the highest CFE (85%) among all specimens during direct axial loading, followed by the specimen H-C-F (81%). The lowest value was observed in H-A-F (61%), as shown in Table 2. The CFE is a crashworthiness indicator which represents how stable the energy absorber is during the collision. With high CFE there is less fluctuation of the force leading to less sharp decelerations which is safer for the car occupants. Table 2 shows that in an identical specimen, besides increasing the energy absorption when foam incorporated the tube, it also enhances the CFE of the structure (See Table 3).

Fig. 7 represents the empty double hexagonal tubes in direct axial impact. The initial peak force represents the maximum force.

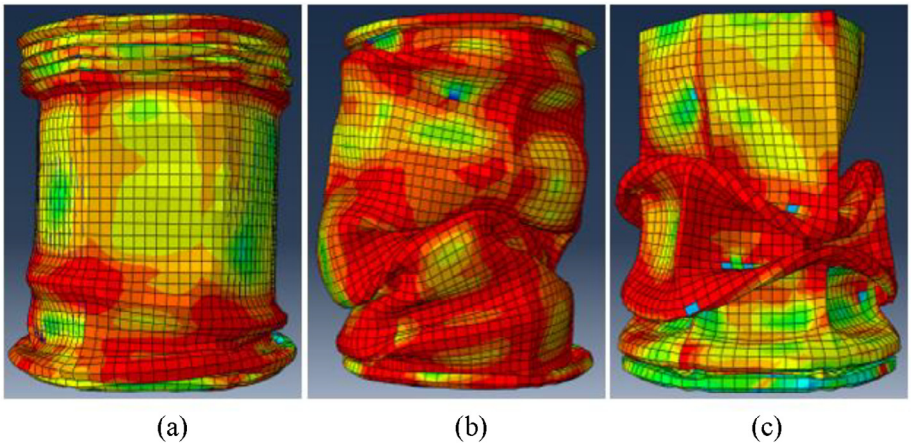

Fig. 5. (a) Foam-filled, (b) partially filled, and (c) empty hexagonal tube.

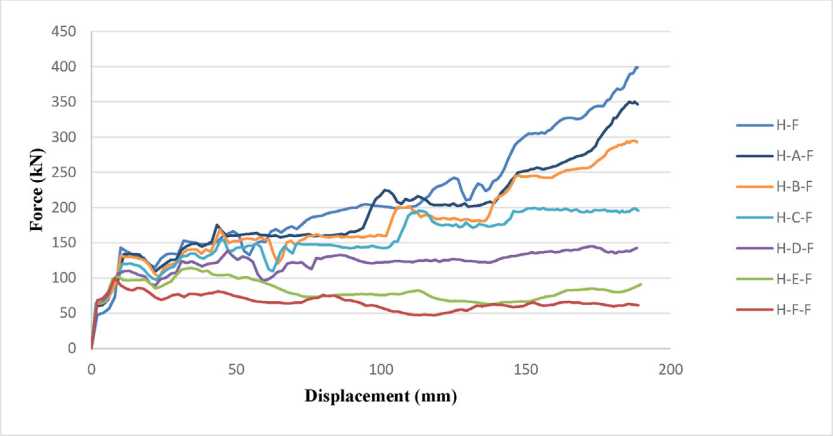

Fig. 6. Force-displacement of the foam-filled double hexagonal tube.

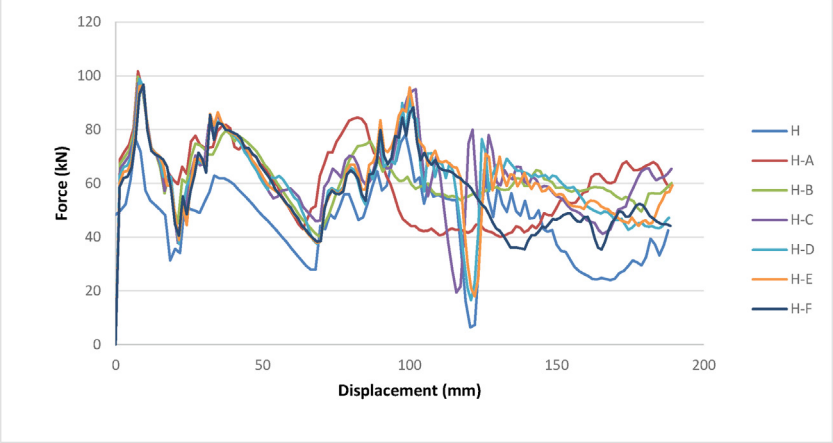

Fig. 7. Force-displacement of an empty double hexagonal tube.

Table 2
Predicted results of the double hexagonal tube for foam-filled and empty tubes in direct loading.

Specimen	outer side (mm)	inner side (mm)	E (kJ)	CFE %	SEA (kJ/kg)	Pmax (kN)	Mass (kg)
H-F	60	0	39.5	64	16.2	399	2.45
H-A-F	60	30	36.2	61	16.7	350	2.17
H-B-F	60	35	33.5	65	16.4	295	2.04
H-C-F	60	40	29	81	15.4	199	1.89
H-D-F	60	45	22.8	85	13.4	145	1.71
H-E-F	60	50	15.1	72	10.1	114	1.5
H-F-F	60	55	12.6	66	9.9	100	1.27
H	60	0	9.8	53	14.4	102	0.68
H-A	60	30	13.3	53	15.7	128	0.85
H-B	60	35	13.2	52	15.0	131	0.88
H-C	60	40	13	50	14.4	136	0.90
H-D	60	45	13.9	50	15.0	139	0.93
H-E	60	50	14.1	51	14.7	143	0.96
H-G	60	55	14.4	49	14.6	148	0.99

The initial force starts rapidly when the striker collides the specimen. This force is needed to form the first fold then, the force decreases. After that, the force begins to increase again to create the second folds and so on. The number of waves (fluctuations) represents the number of folds generated. From Table 2, it is noted when comparing all specimens, the highest initial peak force is found with specimen H-G when the inner tube side is 55 mm. This is because this specimen has the highest stiffness among the other due to its mass. Then the initial force decreases as the tube mass decreases and reaches the lowest value with specimen H which represents the lighter weight. The Fig. 7 illustrates the force–displacement curves of the empty tube specimens has shown that all the specimens had almost similar behaviour with minimal CFE value difference, as shown in Table 2.

Table 3
Predicted results of the double hexagonal tube for foam-filled and empty tubes in 30^0 oblique loading.

Specimen	outer side (mm)	inner side (mm)	E (kJ)	CFE %	SEA (kJ/kg)	Pmax (kN)	Mass (kg)
H-F-O	60	0	21.6	70	8.8	170	2.45
H-A-F-O	60	30	19.6	81	9.0	133	2.17
H-B-F-O	60	35	18.8	77	9.2	133	2.04
H-C-F-O	60	40	16.4	75	8.7	122	1.89
H-D-F-O	60	45	13.7	73	8.0	103	1.71
H-E-F-O	60	50	10	75	6.7	72	1.50
H-F-F-O	60	55	8	71	6.3	61	1.27
H-O	60	0	5	71	7.35	38	0.68
H-A-O	60	30	5.7	68	6.71	46	0.85
H-B-O	60	35	6.2	75	7.05	45	0.88
H-C-O	60	40	7	75	7.78	50	0.90
H-D-O	60	45	7	76	7.53	50	0.93
H-E-O	60	50	6.7	71	6.98	52	0.96
H-G-O	60	55	6.8	68	6.87	54	0.99

Table 4
weightage setting.

	Number of sets, N = 5(5–1)/2 = 10												
											W_j.	w_j.	
	1	2	3	4	5	6	7	8	9	10			
SEA	3	3	3	3							12	12/48	0.25
CFE	3				3	2	2				10	10/48	0.2
SEA-O		2			2			1	2		7	7/48	0.15
CFE-O			2			2		1		2	7	7/48	0.15
Pmax				3			3		3	3	12	12/48	0.25
	Total, Σ G = 48												1

The higher value of the specific energy absorption (SEA) was at the presence of foam especially at a high amount of foam-filled tube and this result encourages researchers and car manufacturers to take foam in their consideration.

4.2. Oblique loading

In case of oblique loading for both empty and foam-filled tubes, the initial peak forces and the amount of the energy absorbed by the structures are lower than those in direct loading. The CFE in case of oblique loading are higher than those of direct in case of the empty tube and this attributes to the lower peak force in case of oblique. The energy absorbed in case of foam-filled tubes are higher than in case of an empty tube and this emphasizes the role of foam. The specific energy absorption in case of foam-filled tubes is higher than those in the empty tubes and higher energy absorbed in case of a higher amount of foam-filled.

4.3. Selection based on crashworthiness performance

The multi-criteria decision making (MCDM) process, the complex proportional assessment method (COPRAS) was chosen to select the best specimen and it is explained in [12,20–21]. In this section, the non-foam filled tubes will be discarded due to their lower crashworthiness performance. The seven foam-filled specimens were studied in both direct and oblique loading. The COPRAS method was used to select the best specimen using the obtained results. The parameters used for selection were SEA, CFE in both direct and oblique loading and the maximum force in case of direct loading. The best specimen represents the one with the higher SEA and CFE with lower possible Pmax.

The method below will be used to calculate the weightage for each criteria W_j.

1. Compare two criteria at a time, the whole comparison sets (N) are equal to N = n(n-1)/2) where n is the number of criteria.
2. The score of 3 will be given to more important, while 2 will be given to less important and 1 will be given to the least.
3. The overall score is determined as $\sum_{i=1}^{m} N_{ij} = W_j$.
4. The weighting factor W_j is calculated by dividing the total score W_j by the overall score $\sum_{j=1}^{m} W_j$ = G table 4.
5. The criterion based on selecting the best structure is the specific energy absorption in both direct (SEA) and oblique (SEA-O), the crushing force efficiency in both direct (CFE) and oblique (CFE-O) and the maximum peak force. The maximum peak force represents the non-beneficial parameters since the higher value the worst effect, while other parameters represent the beneficial parameters, the higher value, the better effect on the structures. The beneficial parameters will be added together and non-beneficial will be added together too. Then sums of beneficial and non-beneficial will be separated as in equations below:

$$S_{+1} = \sum_{j=1}^{n} y_{+ij} \tag{1}$$

$$S_{-1} = \sum_{j=1}^{n} y_{-ij} \tag{2}$$

Where y_{+ij} and y_{-ij} represent beneficial and non-beneficial values.

The higher value of S_{+i} the better the design and the lower value of S_{-i} the better the design.

$$Sum_{positive} = \sum_{i=1}^{m} S_{+i} = \sum_{i=1}^{m} \sum_{j=1}^{n} y_{+ij} \tag{3}$$

$$Sum_{negative} = \sum_{i=1}^{m} S_{-i} = \sum_{i=1}^{m} \sum_{j=1}^{n} y_{-ij} \tag{4}$$

The summation of eqs. (3) and (4) is equal to one.

Table 5
Data of performance indicators in a decision matrix.

Specimen	0.25	0.2	0.15	0.15	0.25
	SEA	CFE	SEA-O	CFE-O	P
H-F	16.2	64	8.83	70	399
H-A-F	16.7	61	9.02	81	350
H-B-F	16.4	65	9.21	77	295
H-C-F	15.4	81	8.7	75	199
H-D-F	13.4	85	8.04	73	145
H-E-F	10.1	72	6.67	75	114
H-F-F	9.9	66	6.29	71	100

Table 6
Weighted normalized decision matrix.

Specimen	SEA	CFE	SEA-o	CFE-o	P
H-F	0.041	0.026	0.023	0.020	0.062
H-A-F	0.043	0.025	0.024	0.023	0.055
H-B-F	0.042	0.026	0.024	0.022	0.046
H-C-F	0.039	0.033	0.023	0.022	0.031
H-D-F	0.034	0.034	0.021	0.021	0.023
H-E-F	0.026	0.029	0.018	0.022	0.018
H-F-F	0.025	0.027	0.017	0.020	0.016

Table 7
Sums of the weighted normalized values.

Specimen		Beneficial		Non-Beneficial	
		si+		si-	
H-F		0.111		0.062	0.251
H-A-F		0.114		0.055	0.286
H-B-F		0.115		0.046	0.339
H-C-F		0.117		0.031	0.503
H-D-F		0.111		0.023	0.690
H-E-F		0.094		0.018	0.877
H-F-F		0.089		0.016	1.000
	∑si+	0.75	∑si-	0.25	3.945

6. The relative significance (Q) can be determined based on relative significance (Q_i). As follows:

$$Q_i = \frac{S_{-min}\sum_{i=1}^{m} S_{-i}}{S_{-i}\sum_{i=1}^{m}\left(\frac{S_{-min}}{S_{-i}}\right)} \quad (5)$$

Where $S_{-min}$is the minimum value of S_{+1}.

So, the higher value of Q_i the better design. The design with the highest relative significance Q_{max} is the best choice.

7. The quantitative utility (U_i) is defined as:

$$U_i = \frac{Q_i}{Q_{max}} \quad (6)$$

The quantitative utility value with 100 is represented as the best design in this method

Tables 5-8 explain the COPRAS selection of the best specimen.

The COPRAS method has chosen the specimen H-D-F with the inner tube side of 45 mm as the best choice followed by the specimen H-F-F while the worst one was the specimen H-F due to having the highest peak force. The selected specimen has good specific energy absorption in both direct and oblique direction, a lower peak force in terms of direct axial loading which is preferred during the collision and the highest CFE in term of direct impact. These performances nominated the specimen to be selected by COPRAS. Hence, the specimen with the outer tube side of 60 mm and inner tube side of 45 mm and foam-filled between the tubes is suitable to be used as an energy absorption member used in the frontal vehicle.

Table 8
Qi and Ui values.

Specimen	Q	U	
H-F	0.127	81.90	7
H-A-F	0.132	85.75	6
H-B-F	0.136	88.07	5
H-C-F	0.148	96.07	4
H-D-F	0.154	100	1
H-E-F	0.150	96.87	3
H-F-F	0.152	98.61	2

5. Conclusion

In this research, the crashworthiness parameters of single and double regular hexagonal tubes subjected to dynamic loading were examined. The research also studied the effect of empty, partially and full foam-filled tubes. 14 different specimens were studied in both direct and oblique loading. The study has considered the maximum peak force, the specific energy absorption (SEA) and the crushing force efficiency (CFE) as crashworthiness parameters to assess the performance of the structure. COPRAS was used to select

the best specimen. COPRAS nominated the specimen H-D-F which has the outer perimeter of 360 mm (hexagonal side of 60 mm) and the inner perimeter of 270 mm (hexagonal side of 45 mm) with partially foam-filled tube. The study also showed that the use of foam had enhanced the energy absorption capability by improving the deformation mode of the filled tube and hence increased in the energy absorption.

CRediT authorship contribution statement

Samer Abdulqadir: Conceptualization, Methodology, Software, Writing - original draft. **Bassam Alaseel:** Data curation, Validation, Writing - review & editing. **M.N.M. Ansari:** Visualization, Supervision, Writing - review & editing.

Declaration of Competing Interest

The authors declare that they have no known competing financial interests or personal relationships that could have appeared to influence the work reported in this paper.

References

[1] J. Fang, Y. Gao, G. Sun, G. Zheng, Q. Li, International journal of mechanical sciences dynamic crashing behavior of new extrudable multi-cell tubes with a functionally graded thickness, Int. J. Mech. Sci. 103 (2015) 63–73.
[2] M. Lu, G. Sun, G. Li, Q. Li, On functionally graded composite structures for crashworthiness, Compos. Struct. 132 (2015) 393–405.
[3] T. Tran, S. Hou, X. Han, N. Nguyen, M. Chau, International Journal of Mechanical Sciences Theoretical prediction and crashworthiness optimization of multi-cell square tubes under oblique impact loading, Int. J. Mech. Sci. 89 (2014) 177–193.
[4] C.W. Isaac, O. Oluwole, Structural response and performance of hexagonal thin-walled grooved tubes under dynamic impact loading conditions, Eng. Struct. 167 (2018) 459–470.
[5] X. Zhang, H. Zhang, Thin-walled structures energy absorption of multi-cell stub columns under axial compression, Thin-Walled Struct. 68 (2013) 156–163.
[6] Y. Zhang, G. Sun, G. Li, Z. Luo, Q. Li, Optimization of foam-filled bitubal structures for crashworthiness criteria, J. Mater. 38 (2012) 99–109.
[7] F. Tarlochan, Design of thin-wall structures for energy absorption applications : design for crash injuries mitigation using magnesium alloy, 24–36, 2013.
[8] S.F. Abdulqadir, Design a new energy absorber longitudinal member and compare with S-shaped design to enhance the energy absorption capability, Alexandria Eng. J. 57 (4) (2018) 3405–3418.
[9] A.A. Nia, M. Parsapour, Thin-Walled Structures Comparative analysis of energy absorption capacity of simple and multi-cell thin-walled tubes with triangular, square, hexagonal and octagonal sections, Thin-Walled Struct. 74 (2014) 155–165.
[10] A. Abdullah, K. Salleh, M. Sahari, F. Samer, J.O. Sameer, Design of octagonal energy absorbing members subjected to dynamic load, Enhance. Crashworth. 2 (2014) 144–152.
[11] Y. L. Ă, Thin-Walled Structures Crashworthiness design of multi-corner thin-walled columns, 46, 1329–1337, 2008.
[12] F. Tarlochan, F. Samer, A. M. S. Hamouda, S. Ramesh, and K. Khalid, Thin-Walled Structures Design of thin-wall structures for energy absorption applications : Enhancement of crashworthiness due to axial and oblique impact forces, 71, 7–17, 2013.
[13] M.F.M. Alkbir, S.M. Sapuan, A.A. Nuraini, M.R. Ishak, Effect of geometry on crashworthiness parameters of natural kenaf fibre reinforced composite hexagonal tubes, J. Mater. 60 (2014) 85–93.
[14] N. Qiu, Y. Gao, J. Fang, Z. Feng, G. Sun, Q. Li, Crashworthiness analysis and design of multi-cell hexagonal columns under multiple loading cases, Finite Elem. Anal. Des. 104 (2015) 89–101.
[15] S. Goyal, C. S. Anand, S. Kumar, and R. Chandmal, Thin-Walled Structures Crashworthiness analysis of foam-filled star shape polygon of thin-walled structure, 144, 2019.
[16] I. Duarte, L. Krstulović-opara, J. Dias-de-oliveira, and M. Vesenjak, Thin-Walled Structures Axial crush performance of polymer-aluminium alloy hybrid foam-filled tubes, 138, 124–136, 2019.
[17] T. U. Eindhoven and D. Version, Improved vehicle crashworthiness design by control of the energy absorption for different collision situations Improved Vehicle Crashworthiness Design by Control of the Energy Absorption for Different Collision Situations, 1999. 2020.
[18] Z. Ahmad, D.P. Thambiratnam, Dynamic computer simulation and energy absorption of foam-filled conical tubes under axial impact loading, Comput. Struct. 87 (3–4) (2009) 186–197.
[19] B. Dehghan-manshadi, H. Mahmudi, A. Abedian, and R. Mahmudi, Materials & Design A novel method for materials selection in mechanical design : Combination of non-linear normalization and a modified digital logic method, 28, 8–15, 2007.
[20] A. Arabameri, M. Yamani, B. Pradhan, A. Melesse, Science of the Total Environment Novel ensembles of COPRAS multi-criteria decision-making with logistic regression, boosted regression tree, and random forest for spatial prediction of gully erosion susceptibility, Sci. Total Environ. 688 (2019) 903–916.
[21] Y. Zheng, Z. Xu, Y. He, H. Liao, Severity assessment of chronic obstructive pulmonary disease based on hesitant fuzzy linguistic COPRAS method, Appl. Soft Comput. J. 69 (2018) 60–71.